

Coordination and Oxidative Addition at a Low-Coordinate Rhodium(η) β -Diiminate Centre

Sander T. H. Willems, Peter H. M. Budzelaar,* Nicolle N. P. Moonen, René de Gelder, Jan M. M. Smits, and Anton W. Gal^[a]

Abstract: The reaction of 14e $[\text{L}_{\text{Me}}\text{Rh}(\text{coe})]$ (**1**; $\text{L}_{\text{Me}} = \text{ArNC}(\text{Me})\text{CHC}(\text{Me})\text{NAr}$, $\text{Ar} = 2,6\text{-Me}_2\text{C}_6\text{H}_3$; $\text{coe} = \text{cis-cyclooctene}$) with phenyl halides and thiophenes was studied to assess the competition between σ coordination, arene π coordination and oxidative addition of a C–X bond. Whereas oxidative addition of the C–Cl and C–Br bonds of chlorobenzene and bromobenzene to $\text{L}_{\text{Me}}\text{Rh}$ results in the dinuclear species $[\{\text{L}_{\text{Me}}\text{Rh}(\text{Ph})(\mu\text{-X})\}_2]$ ($\text{X} = \text{Cl}, \text{Br}$), fluorobenzene yields the dinuclear inverse

sandwich complex $[\{\text{L}_{\text{Me}}\text{Rh}\}_2(\text{anti-}\eta^4\text{:}\eta^4\text{-PhF})]$. Thiophene undergoes oxidative addition of the C–S bond to give a dinuclear product. The reaction of **1** with dibenzo[*b,d*]thiophene (dbt) in the ratio 1:2 resulted in the formation of the σ complex $[\text{L}_{\text{Me}}\text{Rh}(\eta^1\text{-S-dbt})_2]$, which in solution dissociates into free dbt and a

Keywords: coordination modes • N ligands • oxidative addition • rhodium • sandwich complexes

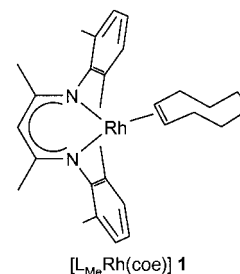
mixture of the mononuclear complex $[\text{L}_{\text{Me}}\text{Rh}(\eta^4\text{-(1,2,3,4-dbt)})]$ and the dinuclear complex $[\{\text{L}_{\text{Me}}\text{Rh}\}_2(\mu\text{-}\eta^4\text{-(1,2,3,4):}\eta^4\text{-(6,7,8,9-dbt)})]$. The latter could be obtained selectively by the 2:1 reaction of **1** and dbt. Reaction of **1** with diethyl sulfide produces $[\text{L}_{\text{Me}}\text{Rh}(\text{Et}_2\text{S})_2]$, which in the presence of hydrogen loses a diethyl sulfide ligand to give $[\text{L}_{\text{Me}}\text{Rh}(\text{Et}_2\text{S})(\text{H}_2)]$ and catalyses the hydrogenation of cyclooctene.

Introduction

Oxidative addition of carbon–heteroatom bonds to coordinatively unsaturated low-valent metal complexes is a key step in catalytic processes such as arylation of alkenes,^[1] cross-coupling reactions^[2] and hydrosulfurisation.^[3] Furthermore it is an important method of forming carbon–metal σ bonds. Usually, a low-valent electron-rich transition metal centre with an empty coordination site is required for oxidative addition.^[4] Examples of oxidative addition of aryl halides to nickel, platinum and palladium^[1, 2, 4, 5] are abundant in the literature; cobalt, rhodium and iridium^[4, 5c, 6c] appear less frequently in this context. Compared to alkyl halides, aryl halides are relatively inert, and the reactivity decreases in the order $\text{ArI} > \text{ArBr} > \text{ArCl} > \text{ArF}$.^[5c]

The 14e β -diiminate complex $[\text{L}_{\text{Me}}\text{Rh}(\text{coe})]$ (**1**; $\text{L}_{\text{Me}} = \text{ArNC}(\text{Me})\text{CHC}(\text{Me})\text{NAr}$, $\text{Ar} = 2,6\text{-Me}_2\text{C}_6\text{H}_3$; $\text{coe} = \text{cis-cyclooctene}$) catalyses the hydrogenation of some “difficult” olefins^[7] and is a precursor for the synthesis of mono- and dinuclear π -arene complexes of the $\text{L}_{\text{Me}}\text{Rh}$ fragment.^[8] Here

we report on the reactivity of $[\text{L}_{\text{Me}}\text{Rh}(\text{coe})]$ with fluorobenzene, chlorobenzene, bromobenzene, diethyl sulfide, allyl methyl sulfide, thiophene and dibenzothiophene. This allowed us to closely examine the balance between π or σ complexation and oxidative addition of the C–X bond ($\text{X} = \text{F}, \text{Cl}, \text{Br}, \text{S}$).



Results and Discussion

Reaction of $[\text{L}_{\text{Me}}\text{Rh}(\text{coe})]$ with bromobenzene and chlorobenzene: When **1** was dissolved in neat bromobenzene the solution turned from dark brown to deep red in two days. The analogous reaction with chlorobenzene required seven days. In the presence of H_2 the reactions with neat bromobenzene and chlorobenzene were complete within one minute. With prior addition of 10 % THF to the phenyl halide the reactions under H_2 were even complete within seconds. For both PhBr and PhCl , oxidative addition to $\text{L}_{\text{Me}}\text{Rh}$ is followed by dimerisation to give five-coordinate $[\{\text{L}_{\text{Me}}\text{Rh}(\text{Ph})(\mu\text{-X})\}_2]$ (**2a** $\text{X} = \text{Br}$, **2b** $\text{X} = \text{Cl}$). The crystal structure of **2a** (Figure 1) shows that each monomeric unit has a square-pyramidal

[a] Dr. P. H. M. Budzelaar, Prof. Dr. A. W. Gal, S. T. H. Willems, N. N. P. Moonen, Dr. R. de Gelder, J. M. M. Smits
Department of Inorganic Chemistry
University of Nijmegen
Toernooiveld 1, 6525 ED, Nijmegen (The Netherlands)
Fax: (+31) 24-3553450
E-mail: budz@sci.kun.nl

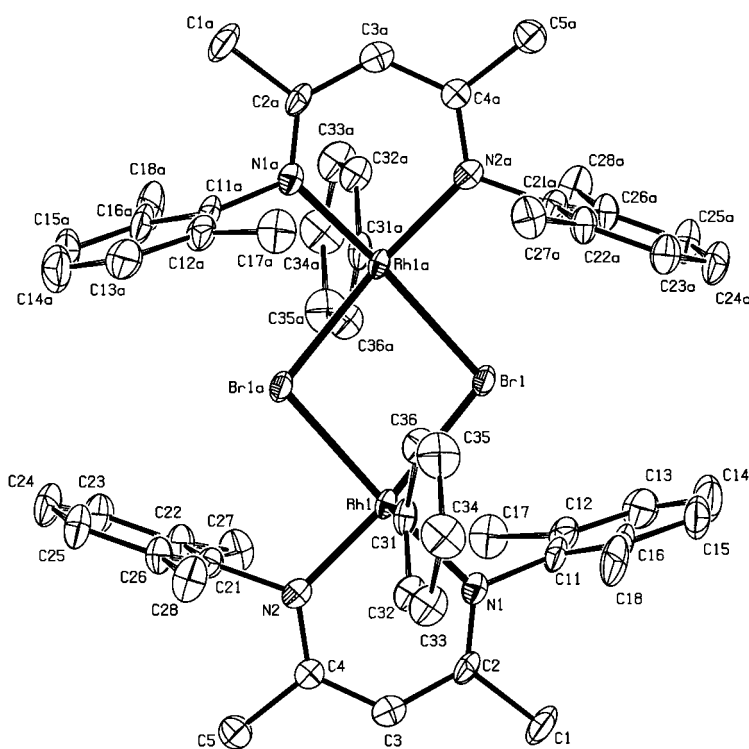


Figure 1. Structure of **2a** (30% ellipsoids; hydrogen atoms and C_6D_6 solvent molecule omitted). Selected bond lengths [Å] and angles [°]: Rh1–C31 2.004(7), Rh1–N1 2.013(6), Rh1–N2 2.026(6), Rh1–Br1a 2.5211(8), Rh1–Br1 2.5255(9), Br1–Rh1a 2.5211(8); C31–Rh1–N1 92.9(3), C31–Rh1–N2 95.7(3), N1–Rh1–N2 90.3(3), C31–Rh1–Br1a 93.4(2), N1–Rh1–Br1a 172.23(17), N2–Rh1–Br1a 93.65(18), C31–Rh1–Br1 95.0(2), N1–Rh1–Br1 93.53(18), N2–Rh1–Br1 168.49(17), Br1a–Rh1–Br1 81.38(3), Rh1a–Br1–Rh1 98.62(3), C2–N1–C11 116.3(6).

coordination environment with the phenyl group in the apical position.

The phenyl groups of the two units are located in a *trans* arrangement, that is, on opposite sides of the Rh_2Br_2 plane. Both phenyl rings are oriented parallel to the Rh–Rh vector. This orientation, which is probably enforced by the bulky 2,6-dimethylphenyl substituents at the nitrogen atoms, would result in steric repulsion between the two phenyl groups in a *cis* arrangement. The Rh^{III} –Br bonds are somewhat shorter than those of related compounds containing the $Rh_2^{III}(\mu-Br)_2$ fragment.^[9] The similarity of the 1H and ^{13}C NMR data of **2a** and **2b** indicates that the chloride-bridged complex **2b** also has the *trans* structure.

To determine whether π coordination of the aryl halide precedes oxidative addition, the reaction was carried out at $-30^\circ C$ in the presence of H_2 in neat phenyl bromide, and NMR spectroscopy showed that $[L_{Me}Rh(coe)(H_2)]$ was formed^[10] but did not react further at that temperature. When the mixture was warmed to $0^\circ C$, **2a** was formed without observable intermediates, that is, a π complex is not formed or rearranges instantaneously to the dinuclear oxidative addition product.

Reaction of $[L_{Me}Rh(coe)]$ with fluorobenzene: Complex **1** was dissolved in fluorobenzene and exposed to an atmosphere of hydrogen. After one minute the fluorobenzene was removed in vacuo. The 1H NMR spectrum showed that **1** had been partly (ca. 60%) converted to a product **3** which has spectroscopic properties consistent with an *anti- μ* -

$\eta^4(1,2,3,4):\eta^4(3,4,5,6)$ inverse sandwich structure.^[8] Carrying out the reaction in PhF/THF (9/1) led to quantitative formation of **3**; an X-ray structure determination confirmed the proposed structure (Figure 2).

The molecule is located on a crystallographic twofold axis, and the fluorobenzene ring is disordered over two orientations. The fluorine substituent avoids the arene “walls” of the diiminate ligand, like the non-disordered toluene molecule in $[(L_{Me}Rh)_2(\mu-\eta^4:\eta^4\text{-toluene})]$.^[8] Because of the disorder in the X-ray structure of **3**, a detailed comparison of geometrical parameters with those of the toluene complex is not possible. However, some similar features can be distinguished: the loss of planarity of the fluorobenzene ring (the deviations from planarity are 0.152(7), 0.072(7), and 0.265(8) Å for the three pairs of symmetry-related atoms) and the localisation of

the single bonds in the arene ring (C31–C32, C31a–C32a and C33–C33a).

When **1** was treated with fluorobenzene/THF (9/1) for 30 s, followed by evaporation of the solvents and immediate dissolution of the resulting solids in $[D_8]THF$ at $-50^\circ C$, the main component was the mononuclear η^4 -fluorobenzene complex **4**. On warming to room temperature, **4** completely disproportionated into the inverse sandwich complex **3**. This behaviour is analogous to that observed for the benzene, toluene, xylene and mesitylene complexes.^[8]

The 1H and ^{13}C NMR spectra of **3** and **4** show effective C_{2v} symmetry of the diiminate ligand; this indicates a highly fluxional fluorobenzene ligand, as was found for the benzene, toluene and *m*-xylene complexes.^[8] The chemical shifts of the fluorobenzene moiety in **3** agree with those calculated for its solid-state $\mu-\eta^4:\eta^4$ structure from intrinsic chemical shifts of other arene complexes.^[8] Similarly the chemical shifts of **4** agree with those calculated for a mononuclear η^4 structure with the F atom on an uncoordinated C atom.^[11]

Mechanistic aspects: Reaction of **1** with pure arenes (benzene, toluene, phenyl halides) is relatively slow (hours to days). Treatment with H_2 accelerates the reaction considerably, and this suggests that generation of a “naked” $12e L_{Me}Rh$ species is rate-limiting. However, formation of the fluorobenzene complex is much slower than the previously observed formation of the toluene complex,^[8] and addition of THF accelerates the reaction considerably. This suggests that coordination of a solvent molecule is important, and that

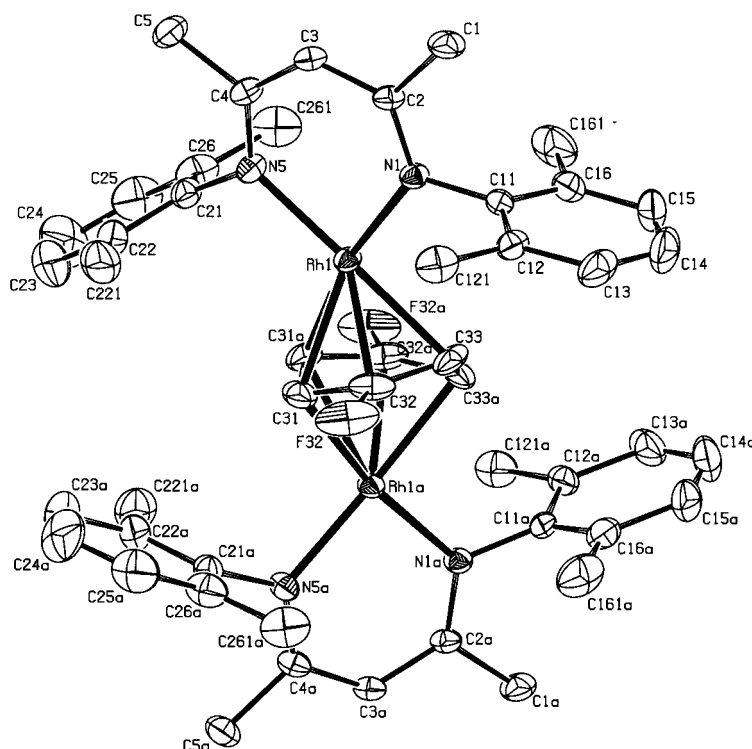


Figure 2. Structure of **3** (30% ellipsoids; hydrogen atoms omitted). Selected bond lengths [Å] and angles [°]: Rh1–N1 2.006(3), Rh1–C32 2.031(5), Rh1–N5 2.048(3), Rh1–C33 2.205(5), Rh1–C31 2.240(5), Rh1–C31a 2.353(5), C31–C31a 1.379(11), C31–C32 1.429(8), C31–Rh1a 2.353(5), C32–F32 1.331(10), C32–C33 1.407(9), C33–C33a 1.493(13); N1–Rh1–C32 113.16(19), N1–Rh1–N5 90.45(14), N1–Rh1–C33 96.78(16), N5–Rh1–C31 111.48(18), N5–Rh1–C31a 97.51(16), C33–Rh1–C31a 73.44(17), F32–C32–C33 136.7(7), F32–C32–C31 107.6(6); Rh1...C32a 2.879(5), Rh1...C33a 2.937(5). The angle between the Rh–Rh vector and the arene least-squares plane is 71.86(12)°.

the weak donor fluorobenzene is relatively inefficient in this respect. Although oxidative addition of chlorobenzene and bromobenzene in the presence of hydrogen is fast in the absence of THF, the addition of THF still speeds up the reaction considerably. Apparently solvent coordination is important in this case as well. Since fluorobenzene, the weakest π donor, forms a π complex, chlorobenzene and bromobenzene could initially do the same. Apparently, the C–F bond is too strong to be broken, whereas for both chlorobenzene and bromobenzene oxidative addition of the C–X bond is fast. Scheme 1 summarises the observed reactivity of **1** with benzene, toluene and phenyl halides. We cannot exclude variations involving direct oxidative addition of a C–X bond without initial π coordination.

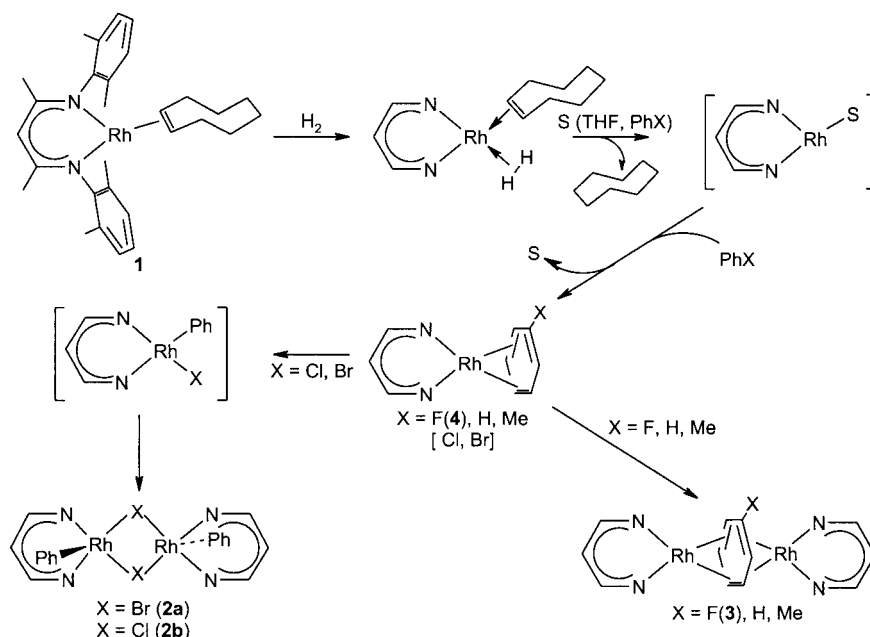
Reactions of $[L_{Me}Rh(coe)]$ with nonaromatic sulfur compounds: Since $[L_{Me}Rh(coe)]$ is

prone to oxidative addition of C–Cl and C–Br bonds, we tested its reactivity towards C–S bonds. Reaction of **1** with two equivalents of the relatively unreactive diethyl sulfide led to substitution of coe and formation of bis(diethyl sulfide) complex **5**. When the reaction was carried with only one equivalent of diethyl sulfide, about half of the starting material was converted into **5**; a mixed coe/sulfide complex was not observed. With one equivalent of the more reactive allyl methyl sulfide we observed formation of complex **6**. 1H NMR data indicate chelation of the allyl methyl sulfide through the sulfur atom and the double bond.

The X-ray crystal structure of **6** (Figure 3) exhibited a complicated disorder, which after extensive refining could best be described as a 4:1:1 mixture of three orientations of the allyl methyl sulfide ligand. Complex **6** appears to be the first example of a

crystallographically characterised allyl alkyl sulfide metal complex.

Reaction of $[L_{Me}Rh(coe)]$ with ethylene sulfide led to a complex mixture of uncharacterizable products.



Scheme 1. Reactivity of **1** with benzene, toluene and phenyl halides.^[10]

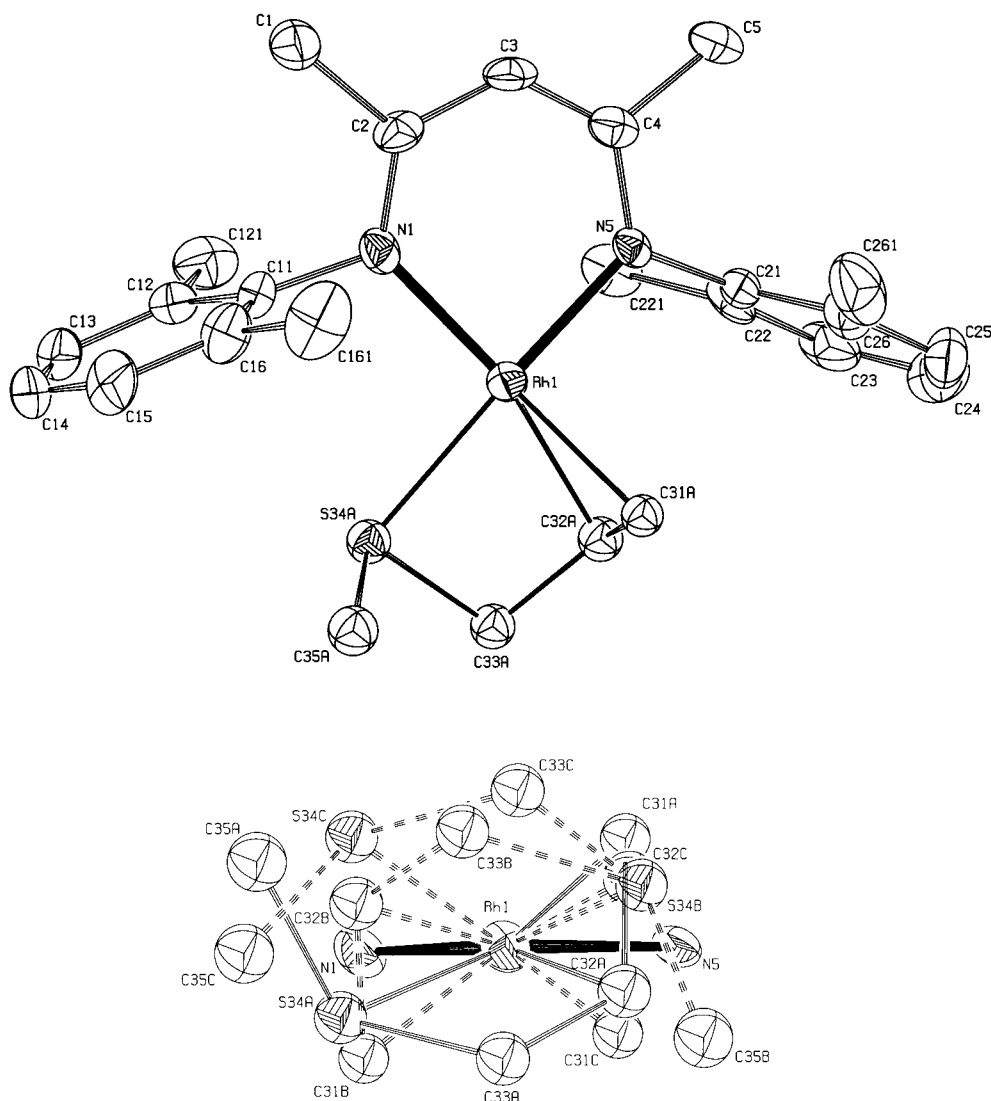
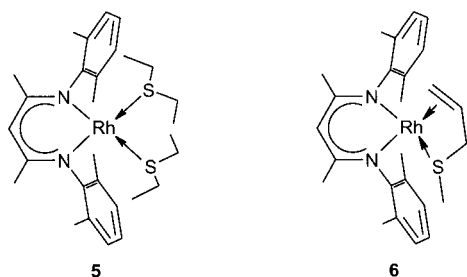
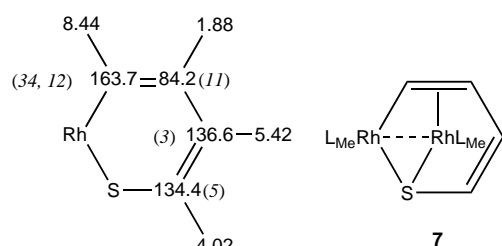


Figure 3. Structure of **6** (30% ellipsoids; hydrogen atoms omitted). The most abundant (66%) of three orientations for the disordered allyl methyl sulfide ligand (top), and the disordered fragment (bottom). Selected bond lengths [Å] and angles [°]: Rh1–N1 2.039(8), Rh1–N5 2.042(7), Rh1–C31A 2.121(12), Rh1–C32A 2.162(12), Rh1–S34A 2.301(4), C31A–C32A 1.41(2), C32A–C33A 1.53(2), C33A–S34A 1.862(14), S34A–C35A 1.820(15); N1–Rh1–N5 90.3(3), N1–Rh1–C31A, 53.5(5), N5–Rh1–C31A 94.4(5), N1–Rh1–C32A 164.3(5), N5–Rh1–C32A 99.5(5), C31A–Rh1–C32A 38.6(6), N1–Rh1–S34A 96.0(3), N5–Rh1–S34A 162.4(2), C31A–Rh1–S34A 87.3(4), C32A–Rh1–S34A 71.2(5), C32A–C33A–S34A 99.7(9), C35A–S34A–C33A 102.5(7), C35A–S34A–Rh1 112.8(6), C33A–S34A–Rh1 86.7(5); Rh1–C32B 2.157(18), Rh1–C31B 2.170(18), Rh1–S34B 2.267(12), C31B–C32B 1.42(3), C32B–C33B 1.53(3), C33B–S34B 1.87(2), S34B–C35B 1.81(2), Rh1–C32C 2.155(18), Rh1–C31C 2.160(18), Rh1–S34C 2.309(13), C31C–C32C 1.41(3), C32C–C33C 1.54(3), C(33C)–S(34C) 1.88(2), S34C–C35C 1.82(2); N5–Rh1–C32B 165.7(11), N5–Rh1–C31B 151.3(14), C32B–Rh1–C31B 38.3(8), N1–Rh1–S34B 165.8(5), C35B–S34B–C33B 103.2(17), C35B–S34B–Rh1 116(2), C33B–S34B–Rh1 86.2(11), N1–Rh1–C32C 162.9(15), N1–Rh1–C31C 155.2(19), C32C–Rh1–C31C 38.3(8), N5–Rh1–S34C 153.4(5), C35C–S34C–C33C 103.0(18), C35C–S34C–Rh1 119(3), C33C–S34C–Rh1 88.5(11).



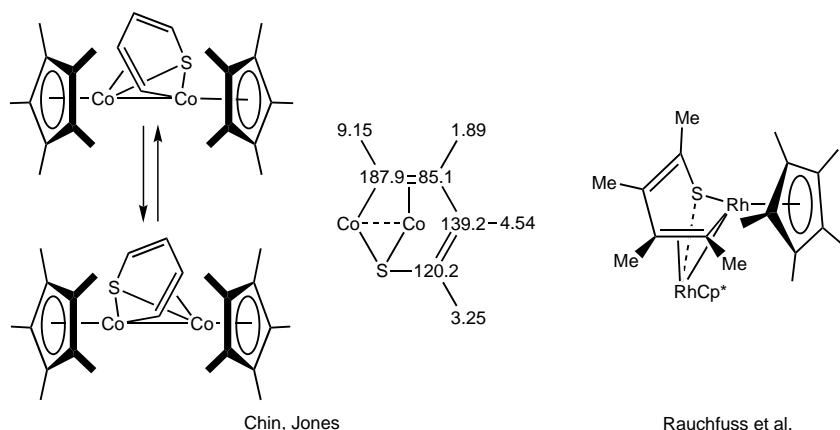
Reactions of $L_{Me}Rh(coe)$ with thiophenes: Oxidative addition and subsequent hydrogenation of thiophenes might be relevant steps in “deep” hydrodesulfurisation (HDS), a field of considerable interest.^[3]

Thiophene readily reacted with $[L_{Me}Rh(coe)]$ in THF at room temperature to give product **7**, which contains two inequivalent asymmetric L_{Me} groups and one C_4H_4S fragment. The four different signals of the C_4H_4S fragment in both the 1H and ^{13}C NMR spectra indicate that it is bound in an unsymmetrical fashion. In particular, the ^{13}C signal at $\delta = 164$ with a large C–Rh coupling (34 Hz, indicative of a Rh–C σ bond) and a smaller coupling (12 Hz, typical of a C=C bond π -coordinated to Rh) suggests it to be a C–S-cleaved thiophene molecule that is π -coordinated to a second Rh atom. These NMR parameters, together with the small Rh couplings to the carbon atoms of the C=C bond next to the sulfur atom, suggest the structure shown in Scheme 2.



Scheme 2. ^1H and ^{13}C chemical shifts ($J_{\text{Rh,C}}$ [Hz]) and the proposed structure for **7**.

A related cobalt compound, structurally characterised by Chin and Jones,^[12] was obtained from the reaction of $[(\text{C}_5\text{Me}_5)\text{Co}(\text{C}_2\text{H}_4)_2]$ with thiophene in benzene at 70°C . The ^1H and ^{13}C NMR shifts of the $\text{C}_4\text{H}_4\text{S}$ fragment in $[(\text{C}_5\text{Me}_5)\text{Co}]_2(\text{C}_4\text{H}_4\text{S})$ are comparable to those of **7**. However, $[(\text{C}_5\text{Me}_5)\text{Co}]_2(\text{C}_4\text{H}_4\text{S})$ is fluxional, whereas **7** is not. This fluxionality was attributed to an interchange of positions between the thiolate sulfur atom and the coordinated double bond, in accordance with the disorder in the bridging $\text{C}_4\text{H}_4\text{S}$ fragment found in the crystal (Scheme 3).



Scheme 3. Previously reported structures related to that of **7**, with relevant NMR parameters.^[13] $\text{Cp}^* = \eta^5\text{-C}_5\text{Me}_5$.

A similar bridged structure was suggested by Rauchfuss et al.^[14] for $[(\text{C}_5\text{Me}_5)\text{Rh}]_2(\text{SC}_4\text{Me}_4)$, a tetramethylthiophene analogue, on the basis of ^1H NMR data and mass spectrometry. This complex was obtained from the slow thermal decomposition of $[(\text{C}_5\text{Me}_5)\text{Rh}]_3(\eta^4;\eta^1\text{-C}_4\text{Me}_4\text{S})_2$ at 100°C . Unfortunately, ^{13}C NMR data were not reported. A dinuclear nickel diphosphane complex with a bonding mode analogous to that of the above cobalt complex shows the same ^1H NMR pattern of chemical shifts but the spread of the thiophene shifts is much smaller (^1H : $\delta = 6.64\text{--}4.62$, ^{13}C : $\delta = 80.8\text{--}70.6$).^[15] Recently, the dinuclear C–S-cleaved 2,5-dimethylthiophene (2,5-Me₂T) rhenium complex $[\text{Re}_2(\text{CO})_7(\mu\text{-}2,5\text{-Me}_2\text{T})]$, obtained by UV photolysis of a hexane solution of $[\text{Re}_2(\text{CO})_{10}]$ and 2,5-dimethylthiophene, was structurally characterised. In this case a $\text{Re}(\text{CO})_4$ moiety was inserted into the C–S bond, and the resulting fragment is η^5 -coordinated to a $\text{Re}(\text{CO})_3$ fragment through the two double bonds and the sulfur atom.^[16]

Reports on insertion of Rh^{I} into the thiophene C–S bond have thus far been restricted to $(\text{C}_5\text{Me}_5)\text{Rh}^{\text{I}}$,^[14, 17, 18] $(\text{Tp}^{\text{Me}_2})(\text{P-Me}_3)\text{Rh}^{\text{I}}$ (Tp^{Me_2} = hydrotris(3,5-dimethylpyrazolyl)borate)^[19] and (triphos) Rh^{I} fragments (triphos = $\text{MeC}(\text{CH}_2\text{P-Ph}_2)_3$).^[20a, 20b] A few Ir^{I} complexes have also been reported to insert into the thiophene C–S bond.^[20a, 20c, 21, 22] $[\text{Ir}(\text{PMe}_3)_3]$, generated from $[\text{Ir}(\text{cod})(\text{PMe}_3)_3]$ (cod = 1,5-cyclooctadiene), inserts into the C–S bonds of thiophene and benzothiophene to give six-membered iridathiacycles.^[21a] Starting from $[(\text{triphos})\text{Ir}(\eta^4\text{-C}_6\text{H}_6)]\text{BPh}_4$, Bianchini et al. inserted (triphos) Ir^{I} into benzothiophene to give a benzoiridathiabenzene complex, which reacted with hydrogen to form a 2-ethylbenzenethiolate complex.^[21b, 21c] In contrast to this iridathiabenzene complex, complex **7** did not react with hydrogen (1 bar, 40°C , 12 h). $[\text{Cp}^*\text{Ir}^{\text{III}}\text{HX}]$ fragments insert into the C–S bonds of thiophene ($\text{X} = \text{H}$; Cl) and benzothiophene ($\text{X} = \text{Cl}$). The resulting complexes then react further with hydrogen (600 psi, 60°C) to give the desulfurised products butane and ethylbenzene.^[22a, 22b] Coordination and reactivity of thiophenes at $(\text{C}_5\text{Me}_5)\text{Ir}^{\text{I}}$ ^[23a] and the reactivity patterns of thiophenes in organometallic complexes^[23b] were recently reviewed.

With respect to hydrodesulfurisation, dibenzothiophene and dimethyldibenzothiophene are more interesting substrates because of their lower reactivity.^[18d] In THF **1** did not react with 4,6-dimethyldibenzo[*b,d*]-thiophene, even under hydrogen. In contrast, the reaction of **1** with two equivalents of dibenzothiophene (dbt) in the absence of hydrogen produced, according to ^1H and ^{13}C NMR data, a mixture of two $\text{L}_{\text{Me}}\text{Rh}$ complexes and free dbt. Repeated crystallisation of the dark brown “mixture” obtained by evaporating the solvent hardly changed its composition.

From the presence in the ^1H NMR spectrum of two pairs of triplets between $\delta = 5.9$ and 6.4 and two pairs of double doublets in the range of $\delta = 1.7\text{--}2.6$, we concluded that in both products dbt is π -coordinated through one or both benzene rings. Moreover, based on the relative intensities of its ^1H NMR signals, the minor product **9** should have a Rh:dbt ratio of 2:1. After several recrystallisation attempts some crystals were obtained which could be characterised by X-ray diffraction. Surprisingly the compound obtained was not a π complex but a bis($\eta^1(\text{S})\text{-dbt}$) complex **8** (Figure 4).

To our knowledge **8** is the first structurally characterised bisdibenzothiophene complex. The $\sigma\text{-S}$ bonding mode has been observed several times for dibenzothiophene^[24a] and $\sigma\text{-S}$ -bonded complexes have been structurally characterised for chromium,^[24b] molybdenum,^[24b, 24c] tungsten,^[24b] manganese,^[24b, 24d] rhenium,^[16, 24e] iron,^[24f] ruthenium^[24g] and iridium.^[24h] S-Coordination of thiophenes in oil^[24c, 24g] and coal^[24f] is believed to be the first step in their catalytic desulfurisation.

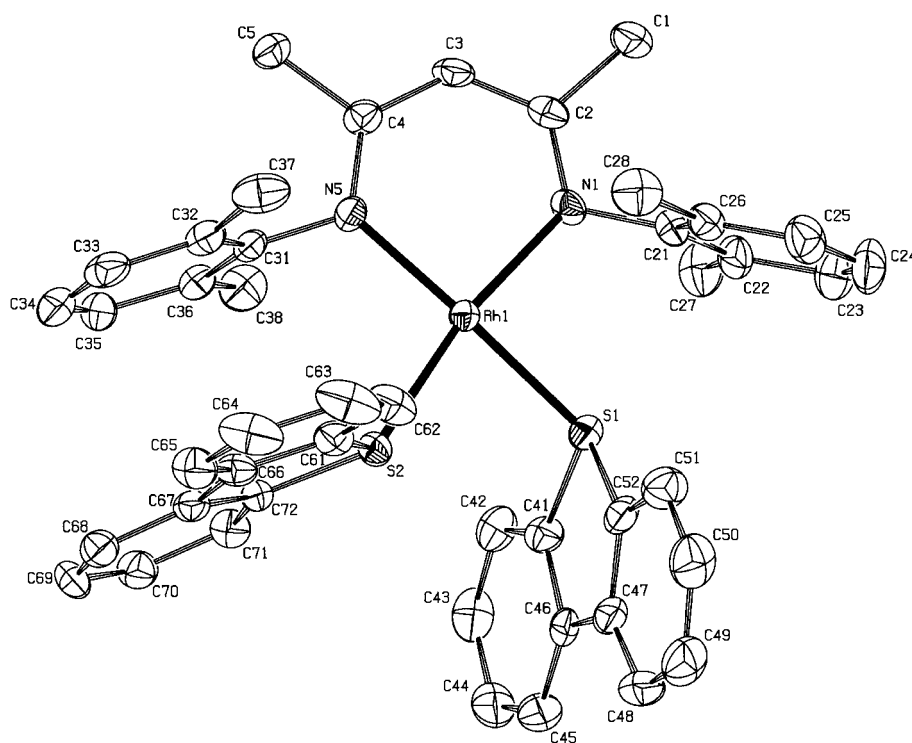


Figure 4. Structure of **8** (30% ellipsoids; hydrogen atoms omitted). Selected bond lengths [Å] and angles [°]: Rh1–N1 2.047(5), Rh1–N5 2.051(6), Rh1–S1 2.2857(19), Rh1–S2 2.2927(18), S1–C41 1.755(8), S1–C52 1.762(8), C41–C46 1.391(10), C46–C47 1.439(11), C47–C52 1.401(10); N1–Rh1–N5 91.4(2), N1–Rh1–S1 88.69(18), N5–Rh1–S1 169.79(17), N1–Rh1–S2 166.40(18), N5–Rh1–S2 98.18(16), S1–Rh1–S2 83.55(7), C41–S1–C52 90.0(4), C41–S1–Rh1 112.7(3), C52–S1–Rh1 121.2(2), C46–C41–S1 113.7(6), C41–C46–C47 111.1(7), C52–C47–C46 112.9(7), C47–C52–S1 111.9(6), Rh1–S1–LSL1 132.41(12), Rh1–S2–LSL2 140.61(13); LSL1 and LSL2 are the least-squares lines constructed through S1–C46–C47 and S2–C66–C67, respectively. The angle between the least-squares plane of the second dbt molecule (S2 and C61–C72) and the least-squares plane of the neighbouring arene ligand (C31–C38) is 2.30(15)°.

As in the other σ -S-dibenzothiophene complexes mentioned, the C–S bond lengths and the C–S–C angles of the dbt moieties in **8** are essentially the same as for free dbt^[25] (C–S 1.76 versus 1.74 Å and C1–S–C12 90.3 vs. 91.5°), and deviation of the dbt moieties from planarity is very small (largest deviation from dbt least-squares plane: 0.080(9) Å). Both dbt ligands in **8** have a pyramidally surrounded sulfur. One of them has a relatively large angle between the Rh–S bond and the vector from the sulfur atom to the midpoint of the bond connecting the benzene rings (Rh1–S2–LSL2 140.61(13)°, see Figure 4), probably to avoid steric contacts with the arene group of the ligand. In the other dbt molecule this angle is only 132.41(12)°, comparable to the values found in the ruthenium (132.0° and 130.1°) and iridium (128.0°) complexes.

Clearly, there is no way to reconcile the solution NMR data with the solid-state structure of **8**. In the hope of gaining more insight into this system, we varied the reaction conditions. When the reaction of [L_{Me}Rh(coe)] with dbt was carried out in a Rh:dbt ratio of 2:1, only the minor product **9** of the two previously observed solution species was formed, and no free dbt was left. In the ¹³C NMR spectrum of **9** all the dbt peaks show coupling to rhodium, that is, both rings are π -coordinated. The crystal structure of **9** confirmed its assignment as a 2:1 Rh:dbt π complex (Figure 5).

The DBT ligand has an *anti*- η^4 : η^4 coordination mode in which the two L_{Me}Rh fragments are coordinated to the four outer carbon atoms of each benzene ring on opposite sides of the dbt plane. Judging by the loss of planarity of the benzene rings of dbt (the outer atoms C104, C105, C110 and C111 show deviations of more than 0.4 Å from the least-squares plane defined by the remaining atoms of DBT), some delocalisation is lost in the benzene rings. Comparison of the bond lengths of *anti*- η^4 : η^4 dbt in **9** with those in free dibenzothiophene^[25] reveals that all bonds of the thiophene ring are slightly shortened, whereas the remaining benzene bonds are all slightly elongated. This suggests that the thiophene ring has gained some delocalisation (Scheme 4), so that the thiophene ring in **9** is more similar to free thiophene.^[27]

π Coordination has been reported or suggested for dibenzothiophene and derivatives in several cases.^[24b, 24h, 28, 29] η^4 Coordination has been suggested only for [Cp*Ir(dbt)].^[28a] All

other examples are supposedly η^6 -dbt complexes, and of these only two are dinuclear complexes, that is, [(CpFe)₂(dbt)]^[29a] and [(CpRu)₂(dbt)]^[29b]. The latter was characterised by X-ray analysis.

The ¹H NMR spectrum of **9** shows two triplets at δ = 6.03 and 5.91 and two double doublets at δ = 1.80 and 1.73. Such rather extreme shifts for aromatic protons have been observed before for η^4 -coordinated species.^[30] Both the ¹H and ¹³C shifts show a fair agreement with the intrinsic shifts calculated earlier for η^4 -arene complexes of L_{Me}Rh; η^6 coordination of the benzene ring would result in rather different chemical shifts, especially for the annellated carbon atoms.^[24h, 28f]

After subtraction of the signals of **9** and free dbt from the ¹H NMR spectrum of a solution of **8**, a set of peaks for **10** (major product) is left that can be fully explained by assuming a 1:1 L_{Me}Rh–dbt π complex. The NMR signals for the uncomplexed benzene ring are not very different from those of free dbt, while those of the complexed ring are similar to those of **9**. Therefore, we propose that dissolution of **8** results in complete redistribution to give a mixture of **9**, **10** and free dbt. Apparently, **8** only crystallises because it has the lowest solubility of all components in the mixture, but in solution the entropy gain associated with dissociation of dbt prevails. This set of equilibria is summarised in Scheme 5.

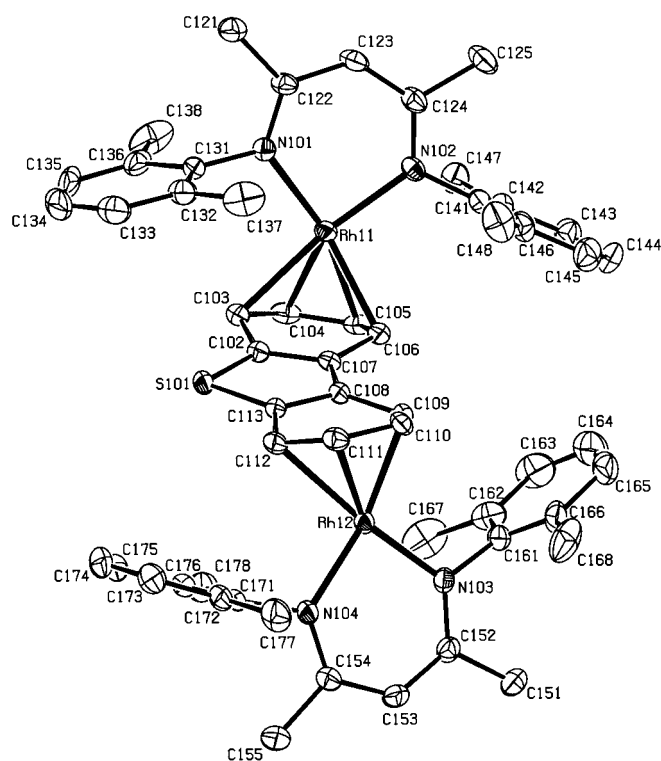


Figure 5. Structure of **9** (30% ellipsoids; hydrogen atoms omitted). Only one of two independent molecules is shown.^[26] Selected bond lengths [Å] and angles [°]: Rh11–N102 2.034(3), Rh11–N101 2.037(3), Rh11–C105 2.124(3), Rh11–C104 2.136(3), Rh11–C106 2.206(3), Rh11–C103 2.301(3), Rh12–N104 2.026(3), Rh12–N103 2.029(3), S101–C102 1.727(3), S101–C113 1.727(3), C102–C107 1.384(4), C102–C103 1.439(5), C103–C104 1.410(5), C104–C105 1.405(5), C105–C106 1.405(5), C106–C107 1.456(4), C107–C108 1.429(5), C108–C113 1.386(4); N102–Rh11–N101 90.42(11), N102–Rh11–C105 105.79(13), N101–Rh11–C105 160.70(13), N102–Rh11–C104 137.34(13), N101–Rh11–C104 122.22(13), N102–Rh11–C106 98.06(12), N101–Rh11–C106 151.52(12), N102–Rh11–C103 171.81(12), N101–Rh11–C103 97.75(12), C102–S101–C113 91.18(16), C107–C102–S101 112.5(3), C102–C107–C108 112.0(3), C113–C108–C107 112.0(3), C108–C113–S101 112.3(3), C123–Rh11–Rh12–C153–C154 125.42(12). The deviations of the atoms C104, C105, C110 and C111 from the least-squares plane defined by the remaining atoms of dbt are 0.405(4), 0.455(4), –0.486(4) and –0.469(4) Å, respectively. The C223–Rh21–Rh22–C253 torsion angle in the second molecule (not shown) is –164.22(13).

Reactivity of **5** towards hydrogen; catalytic hydrogenation:

When diethyl sulfide complex **5** was generated from **1** and Et₂S (ratio Rh:S ≈ 1:4) in [D₈]THF and subsequently subjected to a H₂ atmosphere, hydrogenation of cyclooctene was observed. After all the cyclooctene had been converted, **5** was slowly converted to mainly [L_{Me}Rh(SEt₂)(H₂)] (**11**). Its ¹H NMR spectrum exhibited a sharp 2H doublet at δ = –14.65, which led us to propose an η²-H₂ structure for this

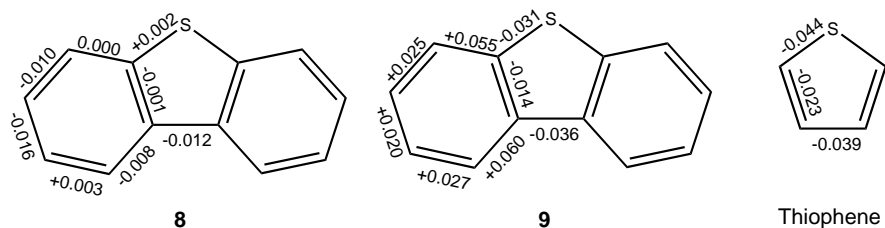
complex, similar to that of [L_{Me}Rh(coe)(H₂)].^[7] A minor product (**12**, ca. 5%) was also observed, which showed a double triplet at δ = –22; this signal could be due to a dinuclear hydrido-bridged rhodium(III) species. The relaxation time *T*₁ of **11** (39.5 ms, room temperature) is comparable to *T*_{1min} of other Rh dihydrogen complexes,^[31] whereas that of **12** (225 ms, room temperature) is typical of a classical hydrido complex. Attempts to isolate a pure sample of either hydrido complex by crystallisation failed due to slow decomposition.

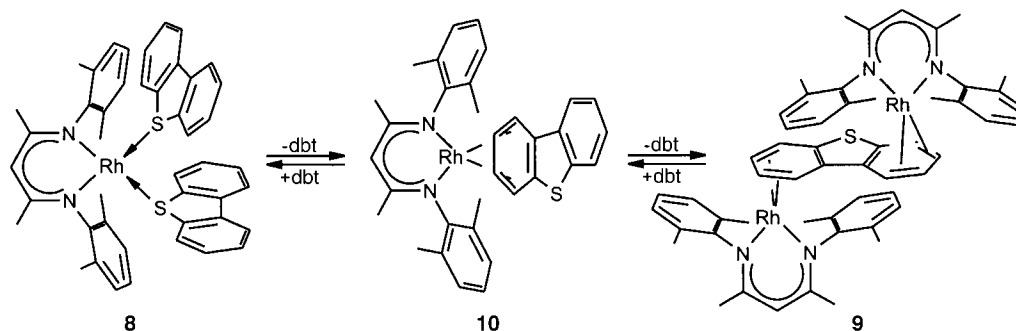
During the entire process starting from **1**, free diethyl sulfide was present and could be clearly distinguished from coordinated diethyl sulfide by NMR spectroscopy. During the hydrogenation of the previously liberated cyclooctene the ratio between coordinated and free Et₂S remained at about 1:1, and only when the dihydrogen complex started to form did the ratio start to change from 1:1 to 1:3. Thus, one of the two coordinated diethyl sulfide molecules in **5** is readily displaced by dihydrogen. Complex **5** is active in the hydrogenation of cyclooctene to cyclooctane under very mild conditions (room temperature, 1 bar H₂), with an initial turnover frequency of around two turnovers per minute. The total turnover number after 3.5 h was 98 (ratio catalyst:coe = 1:110 at room temperature). At this stage the catalyst is almost deactivated. Even though the observed activity is moderate, this result is surprising, as sulfur ligands in general tend to poison hydrogenation catalysts.^[32] In contrast to **1**,^[7] complex **5** does not hydrogenate 2,3-dimethyl-2-butene. This suggests that the mechanism of hydrogenation differs from that of **1**, possibly because one Et₂S ligand remains coordinated during (part of) the catalytic cycle.

Conclusion

The present work clearly demonstrates the subtle balance between complexation and oxidative addition of a C–X bond to a coordinatively unsaturated L_{Me}Rh fragment. With phenyl halides we found a difference between PhF (complexation only) and PhCl and PhBr (oxidative addition). With sulfur compounds, we find examples of σ-S coordination (Et₂S, dbt), σ-S plus π-C=C coordination (allyl methyl sulfide), η⁴-arene coordination (dbt) and oxidative addition (thiophene).

In the case of PhCl and PhBr, the rather slow oxidative addition to [L_{Me}Rh(coe)] in the absence of hydrogen demonstrates that the empty site in this complex is not a sufficient condition for high reactivity in oxidative addition. The L_{Me}Rh fragment has a pronounced tendency to form arene π complexes. Such π complexes could be intermediates in the oxidative addition of phenyl halides and possibly even of thiophene.



Scheme 5. Disproportionation equilibria upon dissolution of **8** in THF.

Experimental Section

Syntheses: All reactions were carried out in an argon atmosphere by using Schlenk techniques. Solvents were distilled under nitrogen from Na/benzophenone prior to use. [L_{Me}Rh(coe)] was prepared according to previously reported methods.^[33]

trans-[{L_{Me}Rh(Ph)(μ-Br)}₂] (2a**):** [L_{Me}Rh(coe)] (0.15 g) was dissolved in bromobenzene (0.5 mL), and dry THF (0.1 mL) was added, after which the solution was subjected to a dihydrogen atmosphere for one minute. Then the excess bromobenzene and the THF were removed in vacuo, and the remaining solids were washed with dry hexane (3 mL). Recrystallisation from hot toluene yielded small red-purple crystals (0.115 g, 70%). Crystals suitable for X-ray analysis were obtained by slow crystallisation from C₆D₆. Elemental analysis calcd (%) for C₅₄H₆₀N₄Br₂Rh₂ (1130.72): C 57.36, H 5.35, N 4.95; found: C 57.95, H 5.35, N 5.02; ¹H NMR (200.13 MHz, 25 °C, C₆D₆): δ = 7.04 (m, 22H; *m, p* and Ph *o, m, p*), 5.37 (s, 2H; *3*), 2.27 (s, 12H; *o* (opposite to Ph)), 1.57 (s, 12H; *o'* (on Ph side)), 1.32 (s, 12H; *I*); ¹³C{¹H} NMR (100.62 MHz, 25 °C, C₆D₆): δ = 156.7 (2), 148.8 (*i*), 139.0 (Ph *i*), 134.3 (*o*), 132.7 (*o'*), 126.2 (Ph *o*), 125.5 (*p'*), 124.2 (Ph *m*), (*m, m'*, and Ph *p*, probably under C₆D₆ (br at 128)), 98.9 (3), 23.4 (*I*), 19.5 (*o-Me*), 19.3 (*o'-Me*).

trans-[{L_{Me}Rh(Ph)(μ-Cl)}₂] (2b**):** This compound was prepared in the same way as **2a**, but with chlorobenzene instead of bromobenzene. Yield 0.10 g (62%) of red-purple crystals. Elemental analysis calcd (%) for C₅₄H₆₀N₄Cl₂Rh₂ (1041.81): C 62.25, H 5.81, N 5.38; found: C 62.37, H 5.77, N 5.32; ¹H NMR (200.13 MHz, 25 °C, [D₈]THF): δ = 6.98–6.43 (m, 22H; *m, p* and Ph *o, m, p*), 5.52 (s, 2H; *3*), 2.49, 2.16 (s, 12H each, *o, o'*), 1.59 (s, 12H; *I*); ¹³C{¹H} NMR (50.32 MHz, 25 °C, [D₈]THF): δ = 157.32 (2), 149.28 (*i*), 139.4 (Ph *i*), 134.75 and 133.32 (*o, o'*), 130.55 (Ph *p*), 129.30 and 128.07 (*m, m'*), 126.42 (Ph *o*), 125.98 (*p*), 124.30 (Ph *m*), 99.25 (3), 23.50 (1), 19.78 and 19.41 (*o-Me, o'-Me*).

[{L_{Me}Rh}₂(anti-μ-η⁴-η⁴-C₆H₅F)] (3**):** [L_{Me}Rh(coe)] (0.278 g, 0.54 mmol) was dissolved in dry fluorobenzene (2 mL), dry THF (0.05 mL) was added and the reaction mixture was placed in a dihydrogen atmosphere for 1 min. Then the solvents were removed in vacuo and the resulting dark red residue was recrystallised from warm THF (2–3 mL). A dark purplish red microcrystalline powder was obtained (0.13 g, 53%). Recrystallisation from THF yielded a few small crystals, one of which was used for X-ray analysis. Elemental analysis calcd (%) for C₄₈H₅₅N₄Rh₂F (912.801): C 63.16, H 6.07, N 6.14; found: C 63.06, H 6.17, N 6.06; ¹H NMR (500.13 MHz, 25 °C, [D₈]THF): δ = 6.97 (d, *J* = 8 Hz, 8H; *m*), 6.86 (t, *J* = 8 Hz, 4H; *p*), 4.89 (s, 2H; *3*), 3.53 (m, 1H; PhF *p*), 2.07 (s, 24H; *o-Me*), 1.55 (td, *J*₁ = 2, *J*₂ = 5 Hz, 2H; PhF *m*), 1.43 (s, 12H; *I*), 0.92 (dd, *J*₁ = 2, *J*₂ = 5 Hz, 2H; PhF *o*); ¹³C{¹H} NMR (125.76 MHz, 25 °C, [D₈]THF) δ = 158.09 (2), 156.56 (*i*), 133.47 (*o*), 129.66 (*m*), 126.27 (*p*), 99.74 (3), 69.57 (small, t, ⁴*J*_{C,F} = 3 Hz; PhF *p*), 63.74 (td, ³*J*_{C,F} = 6, *J*_{C,Rh} = 2 Hz; PhF *m*), 50.68 (dt, *J*_{C,F} = 16.1, *J*_{C,Rh} = 5 Hz; PhF *o*), 23.67 (*I*), 20.47 (*o-Me*), CF not observed.

[L_{Me}Rh(η⁴-C₆H₅F)] (4**):** [L_{Me}Rh(coe)] (0.91 g) was dissolved in fluorobenzene (0.5 mL), dry THF (0.05 mL) was added and the mixture was subjected to a dihydrogen atmosphere for 1 min. The THF and excess fluorobenzene were immediately removed in vacuo without heating so that the mixture was cooled by the evaporation process. After all the liquid was removed the remaining solids were cooled to –78 °C and at this temperature dissolved in [D₈]THF (0.5 mL). The cooled solution was transferred to a precooled NMR tube, and NMR spectra were recorded at various

temperatures in the range –50 to 25 °C. At low temperature the product mixture contained both the η⁴-aryl and the μ-η⁴:η⁴-sandwich aryl complexes in a ratio of 5:1. Upon warming to room temperature complete conversion of the η⁴-aryl complex to the μ-η⁴:η⁴-sandwich aryl complex **3** was observed. ¹H NMR ([D₈]THF, –50 °C, 500.13 MHz): δ = 7.15 (d, *J* = 7.4 Hz, 4H; *m*), 6.85 (t, *J* = 7.4 Hz, 2H; *p*), 5.44 (t, *J* = 4.7 Hz, 1H; PhF *p*), 4.96 (s, 1H; *3*), 4.16 (m, 2H; PhF *o*), 3.20 (t, *J* = 5.8 Hz, 2H; PhF *m*), 2.30 (s, 12H; *o-Me*), 1.52 (s, 6H; *I*); ¹³C{¹H} NMR ([D₈]THF, –30 °C, 125.76 MHz) δ = 163.6 (d, ¹*J*_{C,F} = 244.1 Hz, CF), 156.5 (*i*), 154.8 (2), 132.3 (*o*), 128.1 (*m*), 124.9 (*p*), 99.9 (3), 84.6 (d, ²*J*_{C,F} = 24.7 Hz, PhF *o*), 80.2 (d, *J*_{C,Rh} = 6.4 Hz, PhF *p*), 78.4 (t, *J*_{C,Rh} = ³*J*_{C,F} ≈ 7.2 Hz, PhF *m*), 22.1 (*I*), 19.0 (*o-Me*).

[L_{Me}Rh(Et₂S)₂] (5**):** [L_{Me}Rh(coe)] (0.24 g) was dissolved in dry THF (2–3 mL), and diethyl sulfide (0.5 mL, ca. 10 equiv) was added with a syringe. After stirring for 30 min the reaction mixture was exposed to a dihydrogen atmosphere for 5–10 min. Then excess diethyl sulfide and THF were removed in vacuo. The solids were extracted with warm hexane (3–4 mL, 60 °C). The solution was concentrated to about 2 mL and stored at –20 °C for a week. A crop of dark crystals was obtained (0.08 g, 30%). Elemental analysis calcd for C₂₉H₄₅N₂RhS₂ (588.71): C 59.17, H 7.70, N 4.76; found: C 58.99, H 7.77, N 4.95; ¹H NMR (500.13 MHz, 25 °C, [D₈]THF): δ = 6.95–6.77 (m, 6H; *m, p*), 4.79 (s, 1H; *3*), 2.39 (s, 12H; *o-Me*), 2.47 (q, *J* = 7.4 Hz, 8H; SCH₂), 1.27 (s, 6H; *I*), 1.01 (t, *J* = 7.4 Hz, 12H; SCH₂CH₃); ¹³C{¹H} NMR (50.32 MHz, 25 °C, [D₈]THF): δ = 155.73 (*i*), 155.22 (2), 133.73 (*o*), 128.16 (*m*), 124.21 (*p*), 98.42 (3), 29.49 (SCH₂), 23.76 (*I*), 19.84 (*o-Me*), 13.41 (SCH₂CH₃).

[L_{Me}Rh(η⁴-(S)-η²-C₃H₅SMe)] (6**):** [L_{Me}Rh(coe)] (0.19 g) was suspended in dry pentane (1–2 mL), and allyl methyl sulfide (1 mL) was added with a syringe. The mixture was stirred for 30 min, after which the pentane and excess allyl methyl sulfide were removed by filtration, and the resulting yellow powder was washed with pentane (1 mL). A bright yellow powder was obtained (0.16 g, 88%). A few crystals suitable for X-ray analysis were obtained from a mixture of cyclohexane and toluene by partial evaporation in vacuo and subsequent cooling to –20 °C. Elemental analysis calcd (%) for C₂₅H₃₃N₂RhS (496.52): C 60.48, H 6.70, N 5.64, S 6.46; found: C 60.18, H 6.64, N 5.57, S 6.23; ¹H NMR (400.14 MHz, 25 °C, [D₈]THF): δ = 7.02 and 6.97 (d, *J* = 7.4 Hz, 2 × 1H; *m, m'*), 6.95 and 6.93 (d, *J* = 7.9 Hz, 2 × 1H; *m'', m'''*), 6.82 and 6.80 (t, *J* = 7.4 Hz, 2 × 1H; *p, p'*), 4.94 (s, 1H; *3*), 3.78 (ddd, ²*J*_{H,H} = 13, *J*₂ = 5.6, *J*₃ = 1.6 Hz, 1H; CH₂S), 3.05 (dd, ³*J*_{trans} = 11, *J*₂ = 2.6 Hz, 1H; CH=CH₂), 2.78 (brd, ²*J*_{H,H} = 13 Hz, 1H; CH₂S), 1.83 (m, 1H; CH=CH₂), 1.71 (brd, ³*J*_{cis} ≈ 5 Hz, 1H; CH=CH₂), 2.42, 2.33, 2.27, 2.11 (s, 3H each; *o-Me, o'-Me, o''-Me, o'''-Me*), 1.56 and 1.43 (s, 3H each, *I, I'*), 0.96 (d, *J* = 1.6 Hz; SMe); ¹³C{¹H} NMR (50.32 MHz, 25 °C, [D₈]THF): δ = 157.52, 155.92 (*i, i'*), 154.16, 150.65 (2, 2'), 132.95, 132.57, 132.47, 132.17 (*o, o', o'', o'''*), 128.58, 128.36, 128.23, 128.09 (*m, m', m'', m'''*), 124.72, 124.26 (*p, p'*), 97.82 (d, *J*_{Rh,C} = 2.7 Hz, 3), 55.74 (d, *J*_{Rh,C} = 16.2 Hz, CH=CH₂), 48.85 (d, *J*_{Rh,C} = 3.6 Hz, CH₂S), 41.33 (d, *J*_{Rh,C} = 9.9 Hz, CH=CH₂), 24.02, 22.72 (*I, I'*), 19.82, 19.65, 19.28, 18.76 (*o, o', o'', o''' Me*), 18.88 (SMe).

[{L_{Me}Rh}₂(C₄H₅S)] (7**):** [L_{Me}Rh(coe)] (0.16 g) was suspended in dry hexane (1–2 mL), and thiophene (0.5 mL) was added with a syringe with vigorous stirring. After stirring for 30 min at room temperature, the mixture was cooled to –20 °C. After a night in the freezer a brown microcrystalline powder was obtained, which was filtered and washed with hexane (0.056 g, 40%). Elemental analysis calcd (%) for C₄₆H₅₄N₄Rh₂S (900.83): C 61.33, H 6.04, N 6.22, S 3.56; found: C 59.48, H 6.09, N 5.93, S 3.38; ¹H NMR (500.13 MHz, 25 °C, [D₈]THF): δ = 8.44 (t, *J*₁ = 5.1 Hz, *J*_{Rh,H} = 5.1 Hz, 1H;

RhCH), 7.14–6.55 (m, 12H; *m*, *m'*, *p*), 5.42 (dd, $J_1 = 6.4$ Hz, $J_2 = 5.8$ Hz, 1H; CH=CHS), 5.30 (s, 1H; 3), 5.19 (s, 1H; 3'), 4.02 (d, $J = 6.4$ Hz, 1H; SCH), 1.88 (dd, $J_1 = 5.1$ Hz, 1H; RhCH=CH), 2.46, 2.30, 2.14, 2.09, 2.07, 2.02, 1.70, 1.61 (s, 3H each, $8 \times o$ -Me), 1.50, 1.42, 1.48, 1.07 (s, 3H each, $4 \times I$); ^{13}C { ^1H } NMR (50.32 MHz, 25 °C, $[\text{D}_8]\text{THF}$): $\delta = 163.97$ (dd, $J_{\text{Rh,C}} = 34.4$, $J_{2\text{Rh,C}} = 12.1$ Hz, RhCH=CH), 162.7, 159.11, 157.81, 157.50, 157.12, 154.54, 154.46, 151.66 ($4 \times i$, 4×2), 136.62 (d, $J_{\text{Rh,C}} = 3$ Hz, SCH=CH), 134.40 (d, $J_{\text{Rh,C}} = 5.4$ Hz, SCH), 134.90, 134.62, 133.39, 133.28, 131.10, 130.92, 130.73, 130.04 ($8 \times o$), 129.46, 129.19, 129.03, 128.70, 128.08, 127.92, 127.80, 127.47 ($8 \times m$), 126.14, 125.15, 125.11, 124.17 ($4 \times p$), 100.65 (d, $J_{\text{Rh,C}} = 2.4$ Hz, 3), 99.83 (d, $J_{\text{Rh,C}} = 3.0$ Hz, 3'), 84.24 (d, $J_{\text{Rh,C}} = 10.8$ Hz, RhCH=CH), 25.02, 23.61, 23.52, 22.91, 21.16, 20.78, 20.55, 20.38, 19.52, 18.93, 18.88, 18.21 ($4 \times I$, $8 \times o$ -Me).

[$\text{L}_{\text{Me}}\text{Rh}(\eta^1(\text{S})\text{-dibenzo}[b,d]\text{thiophene})_2$] (8): [$\text{L}_{\text{Me}}\text{Rh}(\text{coe})$] (0.14 g) was dissolved in dry THF (2–3 mL), and a solution of dibenzothiophene (0.1 g, 2 equiv) in THF (2–3 mL) was added. After 30 min of stirring at room temperature the solvent was evaporated. By slow diffusion of hexane into a THF solution of the products some dark brown crystals were obtained. Single-crystal X-ray analysis showed that the compound obtained was the bis(*S*-dibenzothiophene) complex. NMR data could not be obtained because upon dissolution the compound disproportionates into a mixture of π complexes **9** and **10** (see below) and free dibenzothiophene. Elemental analysis calcd (%) for $\text{C}_{45}\text{H}_{41}\text{N}_2\text{RhS}_2$ (776.86): C 69.67, H 5.32, N 3.61; found: C 68.81, H 5.49, 4.34.

[$\text{L}_{\text{Me}}\text{Rh}$] $_{\text{2}}$ (*anti*- μ - $\eta^1(2,3,4):\eta^4(6,7,8,9)$ -dibenzo[*b,d*]thiophene)] (9): [$\text{L}_{\text{Me}}\text{Rh}(\text{coe})$] (0.25 g) was dissolved in dry THF (1–2 mL), and a solution

of dbt (0.05 g, 0.5 equiv) in THF (1 mL) was added. After stirring for 30 min the reaction mixture was evaporated in vacuo and the remaining solids washed with cool hexane. A dark brown powder was obtained (0.12 g, 49%). Recrystallisation from warm THF afforded few crystals suitable for X-ray analysis. Elemental analysis calcd (%) for $\text{C}_{54}\text{H}_{58}\text{N}_4\text{Rh}_2\text{S}$: C 64.80, H 5.84, N 5.60; found: C 64.72, H 5.64, N 5.52; ^1H NMR (500.13 MHz, 25 °C, $[\text{D}_8]\text{THF}$): $\delta = 7.03$ (m) and 6.88 (m) (6H; *m*, *p*), 6.03 (t, $J_1 \approx J_2 = 5$ Hz, 2H; dbt 5, 10), 5.91 (t, $J_1 \approx J_2 = 5$ Hz, 2H; dbt 4, 11), 4.81 (s, 2H; 3), 2.07 and 1.97 (s, 2×6 H; *o*-Me, *o'*-Me), 1.80 (dd, $J_1 = 1$, $J_2 = 6$ Hz, 2H; dbt 3, 12), 1.73 (dd, $J_1 = 1$, $J_2 = 6$ Hz, 2H; dbt 6, 9), 1.39 (s, 6H; *I*); ^{13}C { ^1H } NMR (50.32 MHz, 25 °C, $[\text{D}_8]\text{THF}$): $\delta = 156.5$ (2), 155.6 (i), 135.7 and 134.2 (*o*, *o'*), 128.32 and 128.06 (*m*, *m'*), 124.95 (*p*), 99.97 (3), 80.88 and 79.80 ($2 \times \text{d}$, $J_{\text{Rh,C}} = 8$ Hz, DBT 4, 11, 10, 5), 70.16 and 69.00 (d, $J_{\text{Rh,C}} = 8$ Hz, dbt 3, 12, 6, 9), 21.68 (*I*), 18.92 and 18.56 (*o*-Me); *ipso*-carbon atoms of DBT not found.

[$\text{L}_{\text{Me}}\text{Rh}(\eta^4(1,2,3,4)\text{-dibenzo}[b,d]\text{thiophene})$] (10): Compound **10** always disproportionates partially into **9** and free dbt (see text) and hence cannot be isolated. NMR parameters were obtained from solutions of **8** (see above) by subtracting all peaks belonging to **10** and free dbt. ^1H NMR ($[\text{D}_8]\text{THF}$, 500.13 MHz): $\delta = 7.51$ (dt, $J_1 = 8$, $J_2 = 1$ Hz, 1H; dbt 11), 7.20 (m, $J_1 = 4$, $J_2 = 1$ Hz, 2H; dbt 9, 12), 7.15 (dd, $J_1 = 8$, $J_2 = 4$ Hz, 1H; dbt 10), 7.11 and 7.07 (d, $J = 7$ Hz, 2×2 H; *m*, *m'*) 6.96 (t, $J = 7$ Hz, 2H; *p*), 6.38 and 6.02 (tm, $J_1 \approx 5$ Hz, 2×1 H; dbt 5, 4), 4.92 (s, 1H; 3), 2.51 and 2.25 (dd, $J_1 = 6$, $J_2 = 1$ Hz, 2×1 H; dbt 6, 3), 2.23, 2.10 (s, 2×3 H; *o*-Me, *o'*-Me) and 1.49 (s, 3H; *I*); ^{13}C { ^1H } NMR (50.32 MHz, 25 °C, $[\text{D}_8]\text{THF}$): $\delta = 156.5$ (2), 155.6 (i), 140.24 (d, small, $J = 3$ Hz, dbt 13), 134.77 (d, small, $J = 3$ Hz, dbt 8), 138.7

Table 1. Details of X-ray structure determinations.

Complex	2a	3	6	8	9
crystal colour	dark red	black	light yellow-brown	transparent red-brown	black
crystal shape	rather regular platelet	rather irregular fragment	irregular needle	rather rough platelet	irregular fragment
crystal size [mm]	$0.46 \times 0.23 \times 0.06$	$0.62 \times 0.48 \times 0.31$	$0.40 \times 0.15 \times 0.14$	$0.52 \times 0.48 \times 0.05$	$0.39 \times 0.30 \times 0.18$
empirical formula	$\text{C}_{60}\text{H}_{66}\text{Br}_2\text{N}_4\text{Rh}_2$	$\text{C}_{48}\text{H}_{55}\text{FN}_4\text{Rh}_2$	$\text{C}_{25}\text{H}_{33}\text{N}_2\text{RhS}$	$\text{C}_{45}\text{H}_{41}\text{N}_2\text{RhS}_2$	$\text{C}_{54}\text{H}_{58}\text{N}_4\text{Rh}_2\text{S}$
formula weight	1208.81	912.78	496.50	776.83	1000.92
temperature [K]	293(2)	293(2)	208(2)	293(2)	150(2)
radiation (graphite-monochromated)	$\text{Cu}_{\text{K}\alpha}$	$\text{Mo}_{\text{K}\alpha}$	$\text{Mo}_{\text{K}\alpha}$	$\text{Mo}_{\text{K}\alpha}$	$\text{Mo}_{\text{K}\alpha}$
wavelength [\AA]	1.54184	0.71073	0.71073	0.71073	0.71073
crystal system	triclinic	monoclinic	monoclinic	monoclinic	triclinic
space group	$P\bar{1}$	$C2/c$	$P21/n$	$P21/c$	$P\bar{1}$
unit cell: no. of reflections	25	25	20	25	42762
θ range	40.041–46.732	10.420–13.448	9.346–13.649	10.288–12.843	1.000–27.500
a [\AA]	11.2908(4)	15.2610(12)	7.4020(8)	13.6043(10)	16.31280(10)
b [\AA]	11.5174(3)	23.1415(18)	22.252(3)	12.1878(18)	16.3328(2)
c [\AA]	12.3696(10)	14.0291(13)	14.420(3)	22.693(2)	21.5356(2)
α [$^\circ$]	103.782(3)	90	90	90	89.2817(4)
β [$^\circ$]	111.124(5)	119.578(7)	93.328(7)	101.849(9)	73.4717(4)
γ [$^\circ$]	102.899(3)	90	90	90	60.6073(4)
volume [\AA^3]	1369.83(13)	4308.9(6)	2371.1(6)	3682.4(7)	4736.85(8)
Z , ρ_{calcd} [Mg m^{-3}]	1, 1.465	4, 1.407	4, 1.391	4, 1.401	4, 1.404
absorption coeff. [mm^{-1}]	6.886	0.807	0.821	0.612	0.781
diffractometer	Enraf-Nonius CAD4	Enraf-Nonius CAD4	Enraf-Nonius CAD4	Enraf-Nonius CAD4	Enraf-Nonius CAD4
scan	$\omega/2\theta$ scan	$\omega/2\theta$ scan	ω scan	$\omega/2\theta$ scan	area detector ϕ and ω
$F(000)$	614	1880	1032	1608	2064
θ range for data collection [$^\circ$]	4.09–69.95	2.91–27.47	3.89–27.48	3.06–27.47	1.00–27.50
index ranges	$-12 \leq h \leq 13$ $-13 \leq k \leq 14$ $-15 \leq l \leq 0$	$0 \leq h \leq 19$ $-30 \leq k \leq 0$ $-18 \leq l \leq 15$	$-9 \leq h \leq 0$ $0 \leq k \leq 28$ $-18 \leq l \leq 18$	$-17 \leq h \leq 17$ $0 \leq k \leq 15$ $0 \leq l \leq 29$	$-21 \leq h \leq 21$ $-21 \leq k \leq 21$ $-27 \leq l \leq 27$
reflections collected/unique	5442/5186	5100/4925	5823/5419	8631/8418	42762/21578
R_{int}	0.0899	0.1964	0.1121	0.0751	0.0417
reflections observed [$I_o > 21 \sigma(I_o)$]	4796	4217	2208	4198	14708
absorption correction	semi-emp. ψ scan	semi-emp. ψ scan	semi-emp. ψ scan	semi-emp. ψ scan	–
ψ scan transm. factors	1.773–0.734	1.046–0.958	1.029–0.977	1.157–0.857	–
data/restraints/parameters	5186/0/314	4925/0/259	5419/43/279	8418/0/457	21578/0/1123
GOF on F^2	2.112	1.197	1.039	1.074	1.046
SHELXL-97 weight parameters	0.10000, 0.00000	0.15540, 0.00000	0.07100, 0.00000	0.05820, 7.71600	0.05790, 0.00000
final $R1$, $wR2$ [$I > 2 \sigma(I)$]	0.0925, 0.2369	0.0678, 0.1994	0.0870, 0.1587	0.0748, 0.1439	0.0407, 0.0942
$R1$, $wR2$ (all data)	0.0953, 0.2392	0.0762, 0.2102	0.2379, 0.2101	0.1740, 0.1781	0.0785, 0.1120
largest difference peak and hole [e \AA^{-3}]	4.289 and –3.121	3.149 and –2.453	0.655 and –0.636	0.971, –0.536	0.637 and –0.769
extinction coefficient	0.0104(10)	–	–	–	–

and 134.94 (*o*, *o'*), 128.42 and 128.31 (*m*, *m'*), 124.90 (*p*), 125.07, 123.99, 123.38, and 120.45 (dbt 12, 9, 11, 10), 100.37 (3), 81.99 and 80.91 (d, $J_{\text{Rh,C}} = 8$ Hz, dbt 4, 5), 69.05 and 68.30 (partly under THF, d, $J_{\text{Rh,C}} = 8$ Hz, dbt 3, 6), 21.68 (1), 18.92 and 18.56 (*o*-Me, *o'*-Me). dbt 2 and 7 not found.

[L_{Me}Rh(Et₂S)(H₂)] (11): [L_{Me}Rh(Et₂S)₂] **5** (0.01 g) was dissolved in [D₈]THF (0.5 mL) and exposed to a dihydrogen atmosphere for 18 h. An NMR spectrum of the reaction mixture showed that a dihydrogen complex had been obtained in about 90% yield. Attempts to crystallise the product were unsuccessful; hence, only the NMR data were recorded. ¹H NMR (400.13 MHz, 25 °C, [D₈]THF): δ = 6.99–6.89 (m, 6H; *m*, *p*), 4.96 (s, 1H; 3), 2.32 (s, 6H; *o*-Me), 2.25 (s, 6H; *o'*-Me), 1.80 (q, $J = 7.3$ Hz, 4H; SCH₂), 1.56 (s, 3H; 1), 1.44 (s, 3H; 1'), 0.97 (t, $J = 7.3$ Hz, 6H; SCH₂CH₃), –14.65 (d, $J_{\text{Rh,H}} = 23.8$ Hz, 2H; Rh(*H*₂)); ¹³C {¹H} NMR (50.32 MHz, 25 °C, [D₈]THF): 158.29 (*i*), 157.51 (*i'*), 155.23 (2), 153.81 (2'), 132.7 (*o*), 131.17 (*o'*), 128.32 (*m*), 128.24 (*m'*), 124.56 (*p*), 124.33 (*p'*), 97.94 (3), 34.05 (SCH₂), 23.05 (1), 21.85 (1'), 19.65 (*o*-Me), 19.49 (*o'*-Me), 13.43 (SCH₂CH₃).

Hydrogenation experiments: Olefins (coe and 2,3-dimethyl-2-butene) were dried over Na and then transferred to a cold trap in vacuo prior to use. The catalyst (10–20 mg) was dissolved in THF (1–2 mL), and the olefin (about 100-fold excess relative to the catalyst) was added, after which the mixture was stirred under 1 bar of dihydrogen for 3 h. At intervals of 30 min a sample (1 µL) was taken directly from the reaction vessel and analysed by gas chromatography.

Crystal structure determinations: Crystals were mounted in thin-walled glass capillaries under Ar. Details of all structure determinations are collected in Table 1. Since the glass capillaries prevented accurate descriptions of the crystal shape, semi-empirical absorption corrections^[34] were applied for all crystals except those of **9**. The structures were solved by the PATTY option^[35] of the DIRDIF program system.^[36] Refinements were carried out with the SHELXL-97 package.^[37] All non-hydrogen atoms were refined with anisotropic temperature factors, except for the atoms of the disordered allyl methyl sulfide moiety of structure **6**, which were refined isotropically. The hydrogen atoms were placed at calculated positions and refined isotropically in riding mode. All refinements were performed by full-matrix least-squares methods on F^2 . Geometrical calculations were carried out either with the PLATON-93 program^[38] or with the PARST96 program^[39] and did not reveal unusual geometric features or unusual short intermolecular contacts. Moreover, the calculations revealed no higher symmetry and no solvent-accessible areas. Crystallographic data (excluding structure factors) for the structures reported in this paper have been deposited with the Cambridge Crystallographic Data Centre as supplementary publication nos. CCDC-168217 (**6**), CCDC-168218 (**3**), CCDC-168219 (**8**), CCDC-168220 (**9**) and CCDC-168221 (**2a**). Copies of the data can be obtained free of charge on application to CCDC, 12 Union Road, Cambridge CB2 1EZ, UK (fax: (+44) 1223 336–033; e-mail: deposit@ccdc.cam.ac.uk).

Acknowledgement

We gratefully acknowledge the able assistance of Mr. P. P. J. Schlebos with numerous NMR measurements. X-ray data for **9** were collected on the CCD diffractometer of the national NWO-CW X-ray facility in Utrecht. We thank Johnson Matthey for a generous loan of rhodium chloride.

- G. P. F. Van Strijdonck, M. D. K. Boele, P. C. J. Kamer, J. G. de Vries, P. W. N. M. van Leeuwen, *Eur. J. Inorg. Chem.* **1999**, 1073–1076.
- J. F. Hartwig, *Angew. Chem.* **1998**, 110, 2154–2177; *Angew. Chem. Int. Ed.* **1998**, 37, 2046–2067.
- C. Bianchini, A. Meli, *Acc. Chem. Res.* **1998**, 31, 109–116.
- J. K. Stille, K. S. Y. Lau, *Acc. Chem. Res.* **1977**, 10, 434–442.
- a) L. M. Rendina, R. J. Puddephatt, *Chem. Rev.* **1997**, 97(6), 1735–1754; b) J. K. Stille, *Angew. Chem.* **1986**, 98, 504–519; *Angew. Chem. Int. Ed. Engl.* **1986**, 25, 508; c) V. V. Grushin, H. Alper, *Chem. Rev.* **1994**, 94, 1047–1062.
- a) K. J. Bradd, B. T. Heaton, C. Jacob, J. T. Sampanthar, A. Steiner, *J. Chem. Soc. Dalton Trans.* **1999**, 1109–1112; b) H. F. Haarman, J. M. Ernstring, M. Kranenburg, H. Kooijman, N. Veldman, A. L. Spek, P. W. N. M. van Leeuwen, K. Vrieze, *Organometallics* **1997**, 16, 887–900; c) V. V. Grushin, H. Alper, *Organometallics* **1991**, 10, 1620–1622; d) S. Zecchin, G. Schiavon, G. Pilloni, M. Martelli, *J. Organomet. Chem.* **1976**, 110, C45–C47.
- P. H. M. Budzelaar, N. N. P. Moonen, R. de Gelder, J. M. M. Smits, A. W. Gal, *Eur. J. Inorg. Chem.*, **2000**, 753–769.
- P. H. M. Budzelaar, N. N. P. Moonen, R. de Gelder, J. M. M. Smits, A. W. Gal, *Chem. Eur. J.* **2000**, 6, 2740–2747.
- Seven such bromide-bridged rhodium(III) compounds, of which only one was five-coordinate, were found in the CCDC database, not including the structures with more than two bridging bromide ligands. The average Rh–Br distance is 2.582 Å, and all values lie between 2.489 and 2.670 Å. In general, five-coordinate Rh^{III} complexes are not rare, as they account about 10% of all Rh^{III} structures in the CCDC (the vast majority are six-coordinate). The structure that resembled our structure most was a bromide-bridged rhodium hydrido species: K. Osakada, T. Koizumi, T. Yamamoto, *Bull. Chem. Soc. Jpn.* **1997**, 70, 189–195. Since the hydrido ligands in this structure were not localised, direct comparison of the geometries was not possible.
- For characterisation of **1** see ref. [33], for the characterisation of the hydrido species see ref. [7], and for details of the mononuclear η^4 – π and the dinuclear sandwich complexes of benzene and toluene see ref. [8].
- The NMR parameters calculated for other orientations of the fluorobenzene moiety in **3** and **4** gave large mismatches.
- a) W. D. Jones, R. M. Chin, *Organometallics* **1992**, 11, 2698–2700; b) W. D. Jones, R. M. Chin, *J. Organomet. Chem.* **1994**, 472, 311–316.
- The reported NMR parameters were assigned in analogy to **7**.
- S. Luo, A. E. Skaugset, T. B. Rauchfuss, S. R. Wilson, *J. Am. Chem. Soc.* **1992**, 114, 1732–1735.
- D. A. Vivic, W. D. Jones, *J. Am. Chem. Soc.* **1999**, 121, 7606–7617.
- M. A. Reynolds, I. A. Guzei, R. J. Angelici, *Organometallics* **2001**, 20, 1071–1078.
- a) W. D. Jones, R. M. Chin, *J. Am. Chem. Soc.* **1992**, 114, 9851–9858; b) R. M. Chin, W. D. Jones, *Angew. Chem.* **1992**, 104, 340–341; *Angew. Chem. Int. Ed. Engl.* **1992**, 31, 357–358.
- a) W. D. Jones, L. Dong, *J. Am. Chem. Soc.* **1991**, 113, 559–564; b) L. Dong, S. B. Duckett, K. F. Ohman, W. D. Jones, *J. Am. Chem. Soc.* **1992**, 114, 151–160; c) A. W. Myers, W. D. Jones, S. M. McClements, *J. Am. Chem. Soc.* **1995**, 117, 11704–11709; d) A. W. Myers, W. D. Jones, *Organometallics* **1996**, 15, 2905–2917; e) C. Blonski, A. W. Myers, M. Palmer, S. Harris, W. D. Jones, *Organometallics* **1997**, 16, 3819–3827; f) W. D. Jones, D. A. Vivic, R. M. Chin, J. H. Roache, A. W. Myers, *Polyhedron* **1997**, 16(18), 3115–3128.
- M. Paneque, P. J. Pérez, A. Pizzano, M. L. Poveda, S. Taboada, M. Trujillo, E. Carmona, *Organometallics* **1999**, 18, 4304–4310.
- a) A. Bacchi, C. Bianchini, V. Herrera, M. V. Jiménez, C. Mealli, A. Meli, S. Moneti, M. Peruzzini, R. A. Sánchez-Delgado, F. Vizza, *J. Chem. Soc. Chem. Commun.* **1995**, 921–922; b) C. Bianchini, P. Frediani, V. Herrera, M. V. Jiménez, A. Meli, L. Rincón, R. A. Sánchez-Delgado, F. Vizza, *J. Am. Chem. Soc.* **1995**, 117, 4333–4346; c) C. Bianchini, A. Meli, M. Peruzzini, F. Vizza, P. Frediani, V. Herrera, R. A. Sánchez-Delgado, *J. Am. Chem. Soc.* **1993**, 115, 2731–2742.
- a) H. E. Selnau, J. S. Merola, *Organometallics* **1993**, 12, 1683–1591; b) C. Bianchini, A. Meli, M. Peruzzini, F. Vizza, P. Frediani, V. Herrera, R. A. Sánchez-Delgado, *J. Am. Chem. Soc.* **1993**, 115, 7505–7506; c) C. Bianchini, A. Meli, M. Peruzzini, F. Vizza, S. Moneti, V. Herrera, R. A. Sánchez-Delgado, *J. Am. Chem. Soc.* **1994**, 116, 4370–4381.
- a) D. A. Vivic, W. D. Jones, *Organometallics* **1997**, 16, 1912–1919; b) D. A. Vivic, W. D. Jones, *Organometallics* **1999**, 18, 134–138; c) J. Chen, L. M. Daniels, R. J. Angelici, *J. Am. Chem. Soc.* **1990**, 112, 199–204.
- a) J. Chen, R. J. Angelici, *Coord. Chem. Rev.* **2000**, 206–207, 63–99; b) R. J. Angelici, *Organometallics* **2001**, 20(7), 1259–1275.
- a) R. J. Angelici, *Coord. Chem. Rev.* **1990**, 105, 61–76; b) M. A. Reynolds, I. A. Guzei, B. C. Logsdon, L. M. Thomas, R. A. Jacobson, R. J. Angelici, *Organometallics* **1999**, 18, 4075–4081; c) D. G. Churchill, B. M. Bridgewater, G. Parkin, *J. Am. Chem. Soc.* **2000**, 122, 178–179; d) C. A. Dullaghan, G. B. Carpenter, D. A. Sweigart, D. S. Choi, S. S. Lee, Y. K. Chung, *Organometallics* **1997**, 16, 5688–5695; e) M.-G. Choi, R. J. Angelici, *Organometallics* **1991**, 10, 2436–2442; f) J. D.

- Goodrich, P. N. Nickias, J. P. Selegue, *Inorg. Chem.* **1987**, *26*, 3426–3428; g) S. M. Bucknor, M. Draganjac, T. B. Rauchfuss, C. J. Ruffing, W. C. Fultz, A. L. Rheingold, *J. Am. Chem. Soc.* **1984**, *106*, 5379–5381; h) K. M. Rao, C. L. Day, R. A. Jacobson, R. J. Angelici, *Inorg. Chem.* **1991**, *30*, 5046–5049.
- [25] R. M. Schaffrin, J. Trotter, *J. Chem. Soc. A* **1970**, 1561.
- [26] The asymmetric crystallographic unit consists of two independent molecules which are markedly different. Taking dibenzothiophene as reference, the two molecules are almost identical on one side (with Rh12 and Rh22, respectively) while they show a pronounced difference on the other side (with Rh11 and Rh21, respectively). The whole ligand system has been rotated when comparing the environments of Rh11 and Rh21. The difference in the torsion angles C123–Rh11–Rh12–C153 and C223–Rh21–Rh22–C253 is 9.8°. Since no chemical reasons are apparent, we ascribe the crystallographic difference to packing effects.
- [27] Bond lengths for thiophene derived from microwave studies: B. Bak, D. Christensen, L. Hansen-Nygaard, J. Rastrup-Andersen, *J. Mol. Spectr.* **1961**, *7*, 58–63.
- [28] a) J. Chen, Y. Su, R. A. Jacobson, R. J. Angelici, *J. Organomet. Chem.* **1992**, *428*, 415–429; b) S. C. Hockett, L. L. Miller, R. A. Jacobson, R. J. Angelici, *Organometallics* **1988**, *7*, 686–691; c) S. C. Hockett, R. J. Angelici, *Organometallics* **1988**, *7*, 1491–1500; d) S. S. Lee, Y. K. Chung, S. W. Lee, *Inorg. Chim. Acta* **1996**, *253*, 39–45; e) N. C. Burton, F. G. N. Cloke, P. B. Hitchcock, G. O. Mepsted, C. Newton, H. Patel, *J. Organomet. Chem.* **1995**, *494*, 241–246; f) J. D. Jackson, S. J. Sharon, D. S. Bacon, R. D. Pike, G. B. Carpenter, *Organometallics* **1994**, *13*, 3972–3980.
- [29] a) C. C. Lee, B. R. Steele, R. G. Sutherland, *J. Organomet. Chem.* **1980**, *186*, 265–270; b) C.-M. J. Wang, R. J. Angelici, *Organometallics* **1990**, *9*, 1770–1777.
- [30] The same effect was also observed for several η^4 -coordinated naphthalene complexes: a) H. Schäufele, D. Hu, H. Pritzkow, U. Zenneck, *Organometallics* **1989**, *8*, 396; b) V. S. Leong, N. J. Cooper, *Organometallics* **1988**, *7*, 2058; c) G. P. Zol'nikova, A. S. Peregudov, Yu. F. Oprunenko, G. M. Babakhina, I. I. Kritskaya, D. N. Kravtsov, *Metalloorg. Khim.* **1988**, *1*, 79; d) J. W. Hull, Jr., W. L. Gladfelter, *Organometallics* **1984**, *3*, 326.
- [31] V. I. Bakmutov, C. Bianchini, M. Peruzzini, F. Vizza, E. V. Vorontsov, *Inorg. Chem.* **2000**, *39*, 1655–1660.
- [32] a) J. C. Bayón, C. Claver, A. M. Masdeu-Bultó, *Coord. Chem. Rev.* **1999**, *193–195*, 73–145; b) M. J. H. Russell, C. White, A. Yates, P. M. Maitlis, *J. Chem. Soc. Dalton Trans.* **1978**, 849.
- [33] P. H. M. Budzelaar, R. de Gelder, A. W. Gal, *Organometallics* **1998**, *17*(19), 4121–4123.
- [34] A. C. T. North, D. C. Philips, F. S. Mathews, *Acta Crystallogr. Sect. A* **1968**, *24*, 351.
- [35] P. T. Beurskens, G. Beurskens, M. Strumpel, C. E. Nordman in *Patterson and Pattersons* (Eds.: J. P. Glusker, B. K. Patterson, M. Rossi), Clarendon, Oxford, **1987**, p. 356.
- [36] P. T. Beurskens, G. Beurskens, W. P. Bosman, R. de Gelder, R. O. Garcia-Granda, R. O. Gould, R. Israel, J. M. M. Smits, DIRDIF-96, A Computer Program System for Crystal Structure Determination by Patterson Methods and Direct Methods Applied to Difference Structure Factors, Crystallography Laboratory, University of Nijmegen, The Netherlands, **1996**.
- [37] G. M. Sheldrick, SHELXL-97, Program for the Refinement of Crystal Structures, University of Göttingen: Germany, **1997**.
- [38] A. L. Spek, *Acta Crystallogr. Sect. A* **1990**, *46*, C-34; A. L. Spek, PLATON-93, A Program for Display and Analysis of Crystal and Molecular Structures, University of Utrecht, The Netherlands, **1995**.
- [39] a) M. Nardelli, *Comput. Chem.* **1983**, *7*, 95; b) M. Nardelli, *J. Appl. Crystallogr.* **1995**, *28*, 659.

Received: August 6, 2001 [F3479]